

Spinel LiGa₅O₈ prospects as ultra-wideband-gap semiconductor: band structure, optical properties and doping.

Walter R. L. Lambrecht*

Department of Physics, Case Western Reserve University,
10900 Euclid Avenue, Cleveland, Ohio 44106-7079, USA

LiGa₅O₈ in the spinel type structure is investigated as a potential ultra-wide-band-gap semiconductor. The band structure is determined using the quasiparticle self-consistent *GW* method and the optical properties are calculated at the Bethe Salpeter Equation level including electron-hole interaction effects. The optical gap including exciton effects and an estimate of the zero-point motion electron phonon coupling renormalizations is estimated to be about 5.2±0.1 eV with an exciton binding energy of about 0.4 eV. Si doping as potential *n*-type dopant is investigated and found to be a promising shallow donor.

I. INTRODUCTION

There is a need for ultra-wide-band-gap semiconductors both for optoelectronic and high-power applications. The high-power applications benefit from a large gap because it is found that the breakdown fields scale with the band gap. Recently, there has been a lot of interest in β -Ga₂O₃, because of its gap of ~ 4.9 eV.[1, 2] In spite of such a large gap it can be doped with Si, Ge or Sn to give semiconducting properties. This finding has sparked a world-wide development of this material in epitaxial form. The development of heterojunction devices involving even higher gap (Al_xGa_{1-x})₂O₃ is making rapid progress. For the higher Al-concentrations *n*-type doping is difficult but *p*-type doping appears to be elusive so far even for Ga₂O₃. This is attributed to formation of self-trapped hole polarons, related in turn to high valence band effective masses. While there are some reports of low-level *p*-type doping by means of defect complexes, these remain controversial and the hole mobility is very low. [3, 4] β -Ga₂O₃ also has led to a renewed interest in fundamental properties because of the unusual monoclinic structure with both tetrahedral and octahedral Ga sites.

On the other hand, LiGaO₂ (lithium gallate) has an even wider band gap and was recently also predicted to be *n*-type dopable by Si or Ge. [5, 6] Like Ga₂O₃ bulk crystals can be grown and offer the possibility of homo-epitaxial growth. It has a much simpler wurtzite based crystal structure with all Ga and Li in tetrahedral coordinations and can be thought of as derived from ZnO by replacing the group-II ion Zn by alternating group-I (Li) and group III Ga ions. Further band gap tuning is possible by replacing Ga by Al and Li by Na in the same *Pna*2₁ crystal structure or closely related structures.[7, 8] The anisotropy of the material leads to interesting exciton splittings with large exciton binding energies and recent calculations [9] were found to be in excellent agreement with experiment[10–12] and give an exciton gap of

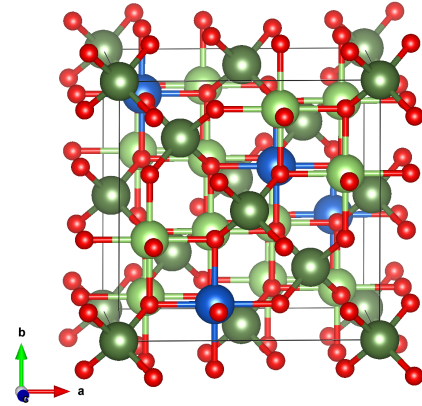


FIG. 1. Crystal structure of LiGa₅O₈, blue spheres Li, light green, octahedral Ga, dark green tetrahedral Ga, red, O

6 eV. It thus appears useful to develop epitaxial growth and doping of this material to pursue it as an active semiconductor material and not merely an optical material.

In the Li-Ga-O ternary system, another stable compound exists with formula LiGa₅O₈. One can think of it as taking 4 LiGaO₂ units and replacing 3 Li with one Ga to maintain the charge balance. However, LiGa₅O₈ is known to have a different crystal structure. It has a cubic spinel-type structure with Ga occurring in both tetrahedral and octahedral sites and Li in octahedral sites.[13] Its structure and related information can be found in [14, 15]. We used the experimental crystal structure from the International Crystallographic Database (ICSD),[16] with cubic lattice constant of 8.203 Å and space group (No. 212) *P*4₃32 or *O*⁶ as shown in Fig. 1. Interestingly, a defective spinel phase also occurs in Ga₂O₃ as a metastable phase and has been labeled the γ -phase [17]. It has recently been observed to occur during certain processing steps in doped β -Ga₂O₃ and a model for how the transition from β to γ phase can proceed via a succession of defect formations was proposed by Hsien-Lien *et al.* [18, 19] Since LiGa₅O₈ is a compound with composition in between Ga₂O₃ and LiGaO₂ it is of interest to determine its band structure and optical properties to assess its potential as UWBG semiconductor. It has pre-

* walter.lambrecht@case.edu

viously been studied as a phosphorescent material when doped with Cr.[20–22] Very recently, LiGa_5O_8 was grown epitaxially and reported to exhibit p -type conduction.[23] The relation to the γ -phase of Ga_2O_3 , which is known to have a higher band gap than the β -phase, provides additional interest. It suggests that adding a small amount of Li may stabilize the γ -phase.

This paper presents results on the electronic band structure using the state-of-the-art quasiparticle self-consistent GW method and also calculates optical properties, including excitonic effects. Since the unit cell already has 56 atoms, (8 formula units) we can already obtain an idea of doping by simply replacing one Ga by a Si. We thus also study a $\text{Li}_4\text{Ga}_{19}\text{SiO}_{32}$ cell with Si placed on either a tetrahedral or octahedral Ga site.

II. COMPUTATIONAL METHODS

The calculations were performed using the QUESTAAL suite,[24] which uses the full-potential linearized muffin-tin orbital method (FP-LMTO) [25] to implement both density functional theory (DFT) and many-body perturbation theory (MBPT) approaches such as Hedin’s GW method for quasiparticle band structures (G for Green’s function and W for screened Coulomb interaction)[26, 27] in a quasiparticle self-consistent version called QSGW, [28, 29] and the Bethe Salpeter Equation (BSE) approach for optical response calculations.[30–32] Specifically, we here use an extension of the QSGW method in which the screened Coulomb interaction is calculated including ladder diagrams, which has been dubbed QSG \dot{W} , [32] and involves solving a BSE equation not just in the $\mathbf{q} \rightarrow 0$ limit for optical response but for the mesh of \mathbf{q} for which $W(\mathbf{q}, \omega)$ is needed. The muffin-tin-orbital basis functions have atom centered spherical harmonic times smoothed Hankel functions as envelope functions [24, 33], which are then replaced in its own and every other sphere by an expansion in spherical harmonics times radial solutions of the Schrödinger equation at a linearization energy and its energy derivative which match in value and slope to the envelope functions. This process is called augmentation. The expansion of the basis function centered on one site about another is carried out by means of structure constants. The basis set angular momentum cut-offs for first and second set of smoothed Hankel function basis sets were $\ell_{max}=3,3$ for Ga and O and 3,2 for Li. Augmentations inside the spheres were carried out up to a higher cut-off of $\ell_{max} \leq 4$. In the QSG \dot{W} calculations 32 valence bands and 4 conduction bands were included in the active space in which the ladder diagrams are evaluated. The PBEsol functional was used for the initial DFT calculations [34]. However, we did not minimize the structure within this functional but used the experimental structural parameters and used the PBEsol only as starting band structure for the subsequent GW calculations. In the QSGW method, the energy dependent self-energy matrix $\Sigma_{ij}(\mathbf{k}, \omega)$ in the basis

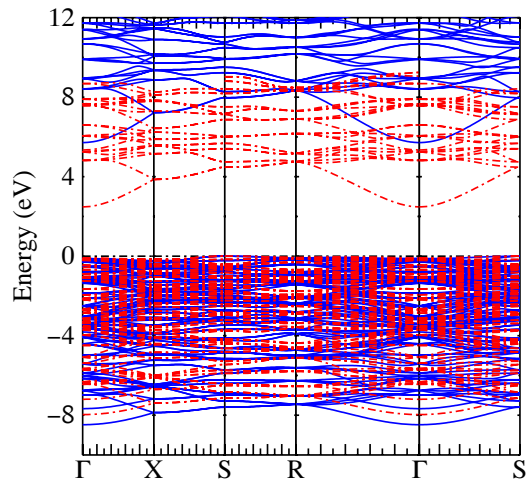


FIG. 2. Band structure of LiGa_5O_8 in GGA (red dashed) and QSG \dot{W} (blue solid) method. The Brillouin zone high-symmetry points follow the convention for a simple cubic structure, $\Gamma = (0, 0, 0)$, $X = (\pi/a, 0, 0)$, $S = (\pi/a, \pi/a, 0)$, (labeled M in [35, 36]), $R = (\pi/a, \pi/a, \pi/a)$

of the Kohn-Sham eigenstates ψ_i is replaced by a Hermitian $\tilde{\Sigma}_{ij}(\mathbf{k}) = \frac{1}{2}\Re[\Sigma_{ij}(\mathbf{k}, \epsilon_i) + \Sigma_{ij}(\mathbf{k}, \epsilon_j)]$ and this acts as a non-local exchange-correlation potential whose difference from the DFT exchange-correlation potential is added to the Kohn-Sham Hamiltonian from which the Σ is calculated in the next iteration until convergence is reached. The self-energy is calculated explicitly up to some maximum energy $\omega_{max} = 3.5$ Ry. The self-energy matrix $\Sigma_{ij}(\mathbf{k}, \omega)$ is approximated by its diagonal above 3.0 Ry with an average value evaluated over the range $3.0 < E < 3.5$ Ry. This procedure is used to facilitate interpolation of the GW bands to other \mathbf{k} -points than the mesh on which the self-energy is calculated explicitly. This is similar to a Wannier function interpolation procedure where the muffin-tin orbitals themselves serve as Wannier functions. For a full description of these technical aspects of the method we refer the reader to Ref. [29].

III. RESULTS

The band structure of LiGa_5O_8 is shown in Fig. 2 as obtained in the GGA and QSGW methods. The conduction band minimum (CBM) occurs at Γ and the top valence band is very flat but with valence band maximum (VBM) at S as shown in Fig. 3. The gap is thus slightly indirect with indirect gap of 5.72 eV and direct gap at Γ at 5.84 eV. The gap is severely underestimated by GGA. Further details on the gap are given in Table I. The difference between the QSG \dot{W} and GGA gap is 3.24 eV and results from a downward shift of the VBM by 1.43 eV and 1.81 upward shift of the CBM. These individual

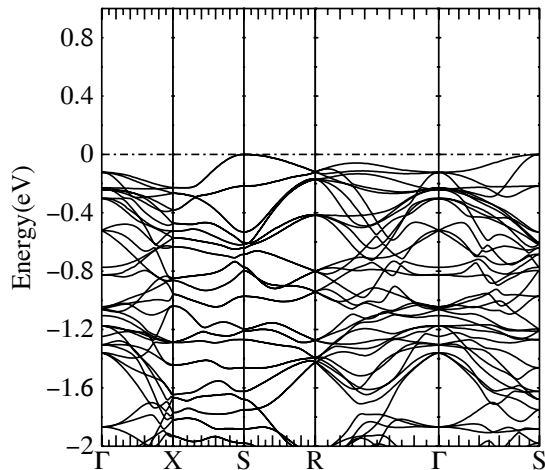


FIG. 3. Zoom in near the valence band maximum of LiGa_5O_8 in QSGW method.

band edge shifts are obtained by directly comparing the DFT and the QSGW band edges relative to the common reference potential, which in the LMTO method is set by an average of the potentials at the muffin-tin radii. It assumes that the self-consistent charge density and the potential apart from the GW -self-energy terms are the same in both cases, which is an excellent approximation.

From Table I we can see that the differences between the QSGW and QSGW gaps in this material is very small. This is somewhat unusual. In most materials studied so far,[32] including the ladder diagrams reduces the GW self-energy by about 10-20 %. For LiGaO_2 , we already found a rather small reduction (5 %) of the self-energy when including ladder diagrams but here the reduction is only 1 %. However, the small effect of ladder diagrams found here may be a result of including an insufficient number of bands in the active space, *i.e.* the space spanned by the $N_v \times N_c \times N_k$ vertical excitation basis states in the two-particle Hamiltonian solved in the BSE step. N_v is the number of occupied states included, N_c the number of empty conduction bands included and N_k the number of \mathbf{k} -points. We estimate the reduction of the self-energy by

$$1 - \frac{E_g^{QSGW} - E_g^{DFT}}{E_g^{QSGW} - E_g^{DFT}}. \quad (1)$$

From the study of standard semiconductors, the guideline is to include the upper set of anion- p -like valence bands and a number of conduction bands up to an equivalent energy above the CBM. Unfortunately, for LiGa_5O_8 including all O- $2p$ bands would require 96 valence bands and including at least one band per Ga in the conduction band would require 20 conduction bands. This presently exceeds the memory allocation requirements we can afford. To check the importance of this convergence issue, we revisited our previous calculations of LiGaO_2 but with

TABLE I. Band gaps of LiGa_5O_8 in eV

	GGA	QSGW	QSGW
indirect ($S - \Gamma$)	2.48	5.75	5.72
direct Γ	2.58	5.87	5.84

a higher number of conduction bands. Instead of using all 52 occupied bands (20 Ga- d like, 8 O- $2s$ and 24 O- $2p$) and only 4 conduction bands which was the default used in [9] we now use 24 valence bands and 12 conduction bands. This gives a gap of 6.737 eV instead of 7.016 eV in [9]. With a QSGW gap of 7.218 eV and GGA gap of 3.314 eV, the Σ_{QSGW} is then estimated to be reduced relative to Σ_{QSGW} by 12 % instead of only 5 %. It is important to note that while this reduces the quasiparticle gap of LiGaO_2 by about 0.3 eV, the same reduction of the screened Coulomb interaction also affects the exciton binding energy. Calculating the exciton gap accurately requires a denser \mathbf{k} mesh. However, for these low lying excitations we can fortunately use a smaller N_v and N_c but need a larger N_k and an extrapolation as function of N_k . This is different from the calculation of the ladder diagrams which involves the overall effect of the screening and requires a higher N_c . Using a similar extrapolation procedure as in [9] for the excitons we then find an extrapolated exciton gap of 6.4 eV. This is in excellent agreement with the result obtained in [9]. However, to compare with experiment, we also need to include a zero-point motion electron-phonon coupling correction, which was there estimated to be -0.4 eV. This finally gave excellent agreement with the experimental value of 6.0 eV for the lowest exciton gap.[12] In conclusion, the main result of that paper of an exciton gap at 6.0 eV and the qualitative analysis of the exciton states presented in that paper holds when we here use a better converged QSGW calculations. However, the quasiparticle gap and the exciton binding energy are both reduced by about 0.3 eV. So, it does represent a correction to those previous results but one which is not so easy to test experimentally as no independent measurements of the exciton binding energy or the quasiparticle gap are available but only the resulting optical gap or exciton energy. This re-analysis of the LiGaO_2 case suggests that the QSGW gap in Table I is still overestimated. Using a reduction factor due to ladders of about 12 % as suggested by the re-evaluation of LiGaO_2 we would obtain an indirect gap of 5.4 ± 0.1 eV and direct gap at Γ of 5.5 eV.

The dielectric function is shown in Fig. 4 in the independent particle approximation (IPA) and the BSE approximation. We can see a significant effect from including the electron-hole interaction effects and excitons with a large exciton binding energy. We caution that the dielectric constant $\epsilon(\omega = 0)$ obtained here is likely overestimated as is the intensity of $\epsilon_2(\omega)$ because of difficulties in calculating the contribution of the self-energy to the velocity matrix elements but the peak positions should be accurate. In this calculation we only used $N_k = 2$ in a

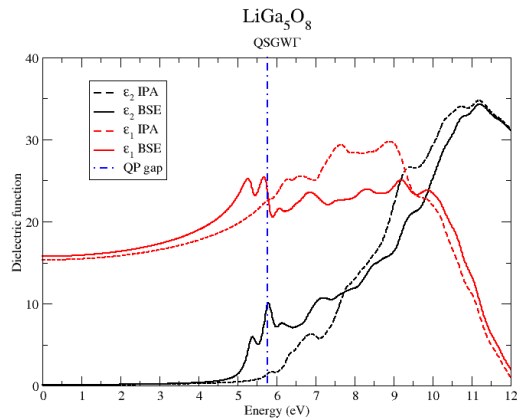


FIG. 4. Real and imaginary part of the dielectric function.

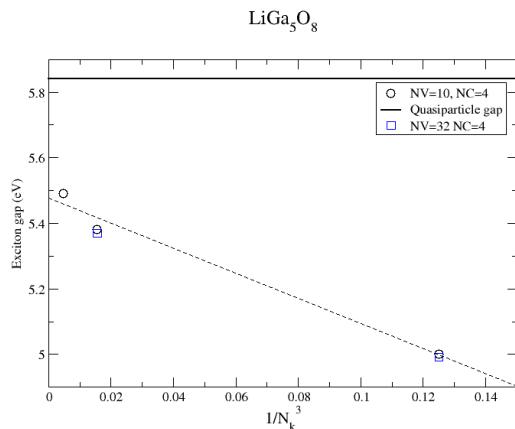


FIG. 5. Exciton gap as function of k -mesh.

$N_k \times N_k \times N_k$ mesh for the BSE equation. To obtain the excitons more accurately, we calculated the lowest exciton for finer k -meshes with $N_k = 4, 6$ but with smaller number of bands 10 valence bands instead of 32 while keeping 4 conduction bands. We can see that reducing the number of valence bands makes a difference of only 0.01 eV with slightly lower gaps obtained with more valence bands included. Extrapolating the gap as function of $1/N_k^3$, *i.e.* the total number of mesh points in the BZ, as we did in [9] we find an extrapolated lowest exciton at 5.48 eV, close to our calculated gap for $N_k = 6$. This would amount to a exciton binding energy of ~ 0.4 eV. The BSE calculations here only include direct transitions. Therefore we deduce the exciton binding energy with respect to the direct gap at Γ . One may expect a similar binding energy for an exciton related to the indirect gap which is ~ 0.1 eV smaller. Neither the quasiparticle gap nor the exciton gap here include electron-phonon coupling renormalization. In LiGaO_2 , the latter was found to be -0.3 ± 0.1 eV. A similar value is expected here

and would reduce our direct gap of Table I from 5.87 to 5.6 ± 0.1 eV (quasiparticle) and 5.2 ± 0.1 eV (exciton) and another 0.1 eV lower for the indirect quasiparticle and exciton gaps. Both the quasiparticle gap and exciton binding energy could be somewhat lower if we assume a larger reduction of \hat{W} relative to W due to ladder diagrams but as mentioned earlier for LiGaO_2 , we expect these two errors to compensate each other and give a similar optical gap. This gap is slightly higher than the gap of 5.0 eV reported [17] for $\gamma\text{-Ga}_2\text{O}_3$.

To evaluate the n -type dopability of the system, we replaced one Ga atom in the 56 atom cell with Si. Fig.6(a) shows the band structure for the tetrahedral Si site after relaxation of the atomic positions keeping the volume of the cell fixed and in the GGA. One can see that the extra valence electron essentially starts filling the conduction band but no levels occur in the gap. The gap in fact slightly increased from 2.58 eV in pure LiGa_5O_8 in the GGA to 2.74 eV. This is partly due to the relaxation. Without relaxation the gap would have decreased slightly to 2.39 eV. The Si contribution to the bands in this figure is indicated by the red color while the background color of the bands without Si contribution is grey. The relaxation is significant. As can be seen in Fig. 7, the nearest neighbor O move inward toward the Si but with also a distortion and symmetry lowering making one Si-O bond longer than the other three. The bond lengths change from 1.776 Å for the Ga-O tetrahedral bond to 1.675 Å (3 bonds) and 1.695 Å (one Si-O) bond. The Ga atoms bonded to these nearest neighbor O atoms then have a larger bond length again by about 0.1 Å than the original octahedral Ga-O bond length of 2.05 Å. In spite of these relaxations there clearly is no deep level formation. This indicates that Si would be a shallow donor and could lead to n -type doping.

We have also calculated Si on an octahedral site with similar results. First, we find that the relaxed total energies were within error bar indistinguishable. So Si is likely to occupy either octahedral or tetrahedral sites with equal likelihood. Secondly, we find no states in the gap in either case, indicating that Si is a shallow donor on both sites as seen in Fig. 6(b). Similar to the tetrahedral case, we find a slight increase in gap due to the Si replacement to 2.688 eV in GGA. Two of the octahedral bonds around Si are 1.814 Å, two are 1.864 Å, and two are 1.784 Å. The Ga-O octahedral bonds in the host are 1.982 Å. Thus, there is again an inward relaxation of nearby O toward the Si.

While we have here only studied the Si doping via the GGA band structure, we expect that the shallow donor character will stay valid at the QSGW level. A similar situation was found recently for LiAlO_2 . [7]

Of course, a full evaluation of doping possibilities will also require a study of native defects and compensation issues. Work along those lines is in progress and will be published elsewhere.

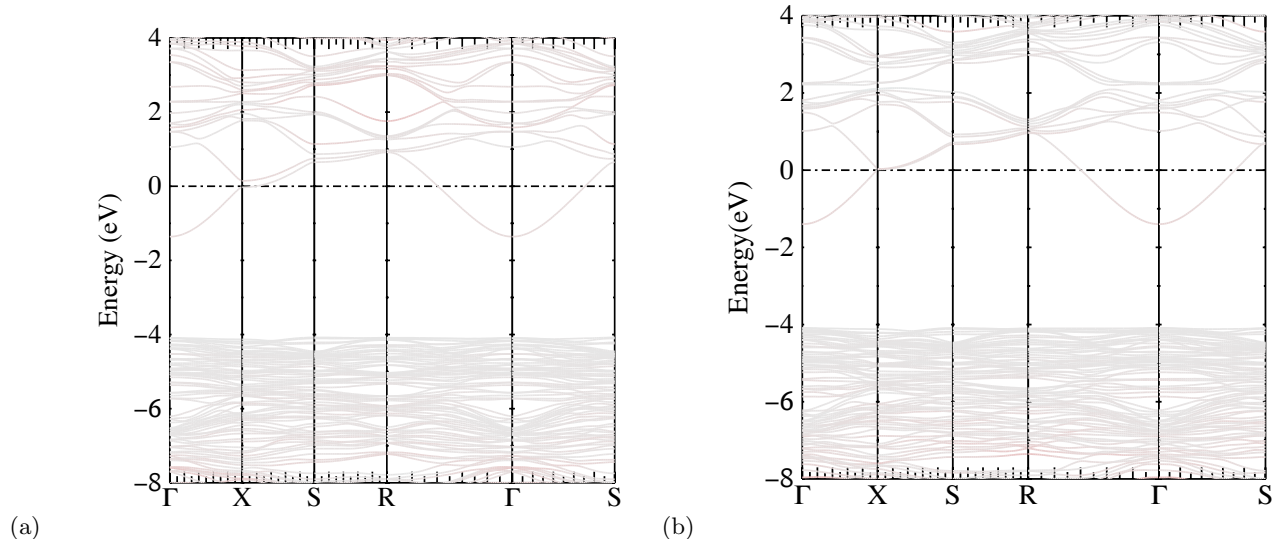


FIG. 6. Band structure of $\text{SiLi}_4\text{Ga}_{19}\text{O}_{32}$ with Si in tetrahedral site (a), octahedral site (b). Red indicates the Si-dopant contribution to the bands, bands without Si are light grey.

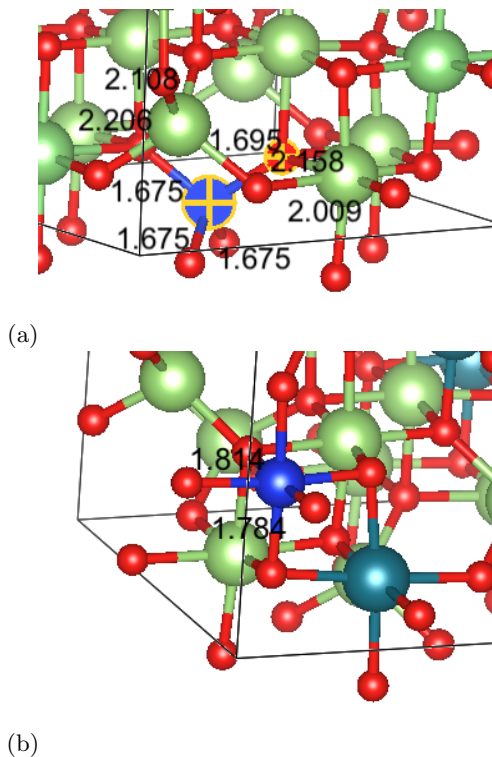


FIG. 7. Bond lengths (\AA) near Si relaxed structure for: (a) tetrahedral, (b) octahedral site. The blue sphere is Si, the green Ga and the teal one is Li. The longest Si-O bond is indicated by the crosses in (a).

IV. CONCLUSION

In summary, LiGa_5O_8 in the spinel type cubic structure is a good candidate UWBG semiconductor. It is predicted to have slightly higher gap than $\gamma\text{-Ga}_2\text{O}_3$ of about 5.3 eV but not as high as LiGaO_2 and appears to be *n*-type dopable by Si on either its tetrahedral or octahedral Ga site. Its cubic structure may have advantages.

ACKNOWLEDGMENTS

This work made use of the High Performance Computing Resource in the Core Facility for Advanced Research Computing at Case Western Reserve University and was supported by the U.S. Air Force Office of Scientific Research (AFOSR) under grant no. FA9550-22-1-0201. I thank Hongping Zhao for communicating her results on epitaxial growth of LiGa_5O_8 prior to publication, which initiated my interest in this material.

Data Availability: The data that supports the findings of this study are available within the article.

Conflicts of Interest The author has no conflicts to disclose.

[1] T. Matsumoto, M. Aoki, A. Kinoshita, and T. Aono, Absorption and Reflection of Vapor Grown Single Crystal Platelets of $\beta\text{-Ga}_2\text{O}_3$, *Jap. J. Appl. Phys.* **13**, 1578

(1974).

[2] K. Sasaki, M. Higashiwaki, A. Kuramata, T. Masui, and S. Yamakoshi, "*{MBE}* grown Ga_2O_3 and its power de-

- vice applications”, *J. Cryst. Growth* **378**, 591 (2013), the 17th International Conference on Molecular Beam Epitaxy.
- [3] Z. Chi, C. Sartet, Y. Zheng, S. Modak, L. Chernyak, C. M. Schaefer, J. Padilla, J. Santiso, A. Ruzin, A.-M. Gonçalves, J. von Bardeleben, G. Guillot, Y. Dumont, A. Pérez-Tomás, and E. Chikoidze, Native defects association enabled room-temperature p-type conductivity in β -Ga₂O₃, *Journal of Alloys and Compounds* **969**, 172454 (2023).
- [4] E. Chikoidze, C. Sartet, H. Mohamed, I. Madaci, T. Tchelidze, M. Modreanu, P. Vales-Castro, C. Rubio, C. Arnold, V. Sallet, Y. Dumont, and A. Pérez-Tomás, Enhancing the intrinsic p-type conductivity of the ultra-wide bandgap Ga₂O₃ semiconductor, *J. Mater. Chem. C* **7**, 10231 (2019).
- [5] A. Boonchun, K. Dabsamut, and W. R. L. Lambrecht, First-principles study of point defects in LiGaO₂, *Journal of Applied Physics* **126**, 155703 (2019).
- [6] K. Dabsamut, A. Boonchun, and W. R. L. Lambrecht, First-principles study of n- and p-type doping opportunities in LiGaO₂, *Journal of Physics D: Applied Physics* **53**, 274002 (2020).
- [7] P. Popp and W. R. L. Lambrecht, Quasiparticle self-consistent *GW* band structures and phase transitions of LiAlO₂ in tetrahedrally and octahedrally coordinated structures, *Phys. Rev. Mater.* **6**, 104605 (2022).
- [8] S. K. Radha, A. Ratnaparkhe, and W. R. L. Lambrecht, Quasiparticle self-consistent *GW* band structures and high-pressure phase transitions of LiGaO₂ and NaGaO₂, *Phys. Rev. B* **103**, 045201 (2021).
- [9] N. Dadkhah, W. R. L. Lambrecht, D. Pashov, and M. van Schilfgaarde, Improved quasiparticle self-consistent electronic band structure and excitons in β -LiGaO₂, *Phys. Rev. B* **107**, 165201 (2023).
- [10] L. Trinkler, A. Trukhin, B. Berzina, V. Korsaks, P. Ščajev, R. Nedzinskas, S. Tuménas, M. Chou, L. Chang, and C.-A. Li, Luminescence properties of LiGaO₂ crystal, *Optical Materials* **69**, 449 (2017).
- [11] L. Trinkler, V. Pankratov, A. Trukhin, B. Berzina, M. Chou, and L. Chang, Anisotropic photoluminescence of β -LiGaO₂ crystal, *Optical Materials* **132**, 112856 (2022).
- [12] S. Tuménas, P. Mackonis, R. Nedzinskas, L. Trinkler, B. Berzina, V. Korsaks, L. Chang, and M. Chou, Optical properties of lithium gallium oxide, *Applied Surface Science* **421**, 837 (2017).
- [13] J. Joubert, M. Brunel, A. Waintal, and A. Durif, Etude cristallographique du gallate de lithium et de sa solution solide avec l’aluminate, *Comptes Rendus Hebdomadaires des Seances de l’Academie des Sciences (1884 - 1965)* **256**, 5324–5326 (1963).
- [14] Data retrieved from Materials Project for LiGa₅O₈ (mp-28146) from database version v2022.10.28.
- [15] A. Jain, S. P. Ong, G. Hautier, W. Chen, W. D. Richards, S. Dacek, S. Cholia, D. Gunter, D. Skinner, G. Ceder, and K. A. Persson, Commentary: The Materials Project: A materials genome approach to accelerating materials innovation, *APL Materials* **1**, 011002 (2013).
- [16] International Crystallographic Data Base, id=33716.
- [17] M. Biswas and H. Nishinaka, Thermodynamically metastable α -, ϵ - (or κ -), and γ -Ga₂O₃: From material growth to device applications, *APL Materials* **10**, 060701 (2022), https://pubs.aip.org/aip/apm/article-pdf/doi/10.1063/5.0085360/16490464/060701_1_online.pdf.
- [18] H.-L. Huang, C. Chae, J. M. Johnson, A. Senckowski, S. Sharma, U. Singiseti, M. H. Wong, and J. Hwang, Atomic scale defect formation and phase transformation in Si implanted β -Ga₂O₃, *APL Materials* **11**, 061113 (2023), https://pubs.aip.org/aip/apm/article-pdf/doi/10.1063/5.0134467/17941303/061113_1_5.0134467.pdf.
- [19] H.-L. Huang, J. M. Johnson, C. Chae, A. Senckowski, M. H. Wong, and J. Hwang, Atomic scale mechanism of β to γ phase transformation in gallium oxide, *Applied Physics Letters* **122**, 251602 (2023), https://pubs.aip.org/aip/apl/article-pdf/doi/10.1063/5.0156009/18006597/251602_1_5.0156009.pdf.
- [20] O. Q. De Clercq, L. I. D. J. Martin, K. Korthout, J. Kusakovskij, H. Vrielinck, and D. Poelman, Probing the local structure of the near-infrared emitting persistent phosphor LiGa₅O₈:Cr³⁺, *J. Mater. Chem. C* **5**, 10861 (2017).
- [21] O. Sousa and I. Carvalho, Theoretical study of the structural, energetic, electronic and magnetic properties of the host matrix LiGa₅O₈ doped with Cr³⁺, *Journal of Solid State Chemistry* **289**, 121472 (2020).
- [22] W. Huang, X. Gong, R. Cui, X. Li, L. Li, X. Wang, and C. Deng, Enhanced persistent luminescence of LiGa₅O₈:Cr³⁺ near-infrared phosphors by codoping Sn⁴⁺, *Journal of Materials Science: Materials in Electronics* **29**, 10535 (2018).
- [23] K. Zhang, V. G. T. Vangipuram, H.-L. Huang, J. Hwang, and H. Zhao, Discovery of a Robust P-Type Ultrawide Bandgap Oxide Semiconductor: LiGa₅O₈, *Advanced Electronic Materials* **n/a**, 2300550, <https://onlinelibrary.wiley.com/doi/pdf/10.1002/aelm.202300550>.
- [24] D. Pashov, S. Acharya, W. R. Lambrecht, J. Jackson, K. D. Belashchenko, A. Chantis, F. Jamet, and M. van Schilfgaarde, Questaal: A package of electronic structure methods based on the linear muffin-tin orbital technique, *Computer Physics Communications*, 107065 (2019).
- [25] T. Kotani and M. van Schilfgaarde, Fusion of the LAPW and LMTO methods: The augmented plane wave plus muffin-tin orbital method, *Phys. Rev. B* **81**, 125117 (2010).
- [26] L. Hedin, New method for calculating the one-particle green’s function with application to the electron-gas problem, *Phys. Rev.* **139**, A796 (1965).
- [27] L. Hedin and S. Lundqvist, Effects of electron-electron and electron-phonon interactions on the one-electron states of solids, in *Solid State Physics, Advanced in Research and Applications*, Vol. 23, edited by F. Seitz, D. Turnbull, and H. Ehrenreich (Academic Press, New York, 1969) pp. 1–181.
- [28] M. van Schilfgaarde, T. Kotani, and S. Faleev, Quasiparticle Self-Consistent *GW* Theory, *Phys. Rev. Lett.* **96**, 226402 (2006).
- [29] T. Kotani, M. van Schilfgaarde, and S. V. Faleev, Quasiparticle self-consistent *GW* method: A basis for the independent-particle approximation, *Phys. Rev. B* **76**, 165106 (2007).
- [30] G. Onida, L. Reining, and A. Rubio, Electronic excitations: density-functional versus many-body Green’s-function approaches, *Rev. Mod. Phys.* **74**, 601 (2002).
- [31] B. Cunningham, M. Grüning, P. Azarhoosh, D. Pashov, and M. van Schilfgaarde, Effect of ladder diagrams on optical absorption spectra in a quasiparticle self-consistent *GW* framework, *Phys. Rev. Materials* **2**, 034603 (2018).

- [32] B. Cunningham, M. Gruening, D. Pashov, and M. van Schilfgaarde, QSGW: Quasiparticle Self consistent GW with ladder diagrams in W (2023), arXiv:2302.06325 [cond-mat.mtrl-sci].
- [33] E. Bott, M. Methfessel, W. Krabs, and P. C. Schmidt, Nonsingular Hankel functions as a new basis for electronic structure calculations, *J. Math. Phys.* **39**, 3393 (1998).
- [34] J. P. Perdew, A. Ruzsinszky, G. I. Csonka, O. A. Vydrov, G. E. Scuseria, L. A. Constantin, X. Zhou, and K. Burke, Restoring the Density-Gradient Expansion for Exchange in Solids and Surfaces, *Phys. Rev. Lett.* **100**, 136406 (2008).
- [35] Bilbao Crystallographic Server, <https://www.cryst.ehu.es>.
- [36] M. I. Aroyo, D. Orobengoa, G. de la Flor, E. S. Tasci, J. M. Perez-Mato, and H. Wondratschek, Brillouin-zone database on the *Bilbao Crystallographic Server*, *Acta Crystallographica Section A* **70**, 126 (2014).